

High-Q microwave photonic filter with self-phase modulation spectrum broadening and third-order dispersion compensation

Dan Zou (邹丹), Xiaoping Zheng (郑小平)*, Shangyuan Li (李尚远),
Hanyi Zhang (张汉一), and Bingkun Zhou (周炳琨)

*Tsinghua National Laboratory for Information Science and Technology,
Department of Electronic Engineering, Tsinghua University, Beijing 100084, China*

*Corresponding author: xpzheng@mail.tsinghua.edu.cn

Received April 24, 2014; accepted June 18, 2014; posted online July 31, 2014

We propose and experimentally demonstrate a scheme of high-Q microwave photonic filter (MPF) using the techniques of self-phase modulation (SPM) spectrum broadening and third-order dispersion (TOD) compensation. The optical pulses from a mode-locking laser are spectrally broadened by the SPM in the highly nonlinear fiber. A wideband optical frequency comb with 365 spectral lines within 10-dB power variation from the highest spectral power is obtained. By applying a cubic phase modulation via a waveshaper, the effect of TOD which broadens the MPF passband is eliminated. The final implemented MPF has a Q-value as high as 296 and a tuning range of 700 MHz.

OCIS codes: 060.5625, 060.4370, 070.1170, 070.2615.

doi: 10.3788/COL201412.080601.

Microwave photonic filter (MPF), the technology of using photonic devices to implement radio frequency (RF) and microwave signal processing, has attracted considerable interest over the past several years. Compared with traditional microwave technologies, it has significant advantages inherent from the photonic technologies, such as high frequency, large bandwidth, low loss, light weight, wide tunability, and immunity to electromagnetic interference^[1,2].

Among all the figure-of-merits to evaluate the performance of a MPF, quality factor (Q-value) is of great concern, as it illustrates the selectivity of the filter. To date, various approaches have been presented to obtain high-Q MPFs in the literature. The first method is based on the optical filter and linear optoelectronic conversion^[3,4]. However, the resolution of the optical filter is quite limited for a microwave filter. The second method is utilizing the narrowband nature of stimulated Brillouin scattering to filter the microwave signals modulated on an optical carrier, which successfully obtains a MPF with Q-value of 678^[5]. This method requires an extra pump light with a stable wavelength relative to the optical carrier and has to avoid the coherent interference. This makes the system sophisticated to be implemented. The third method is based on the mode-locking range of the active harmonic mode-locking fiber ring laser (MLFRL) and Q-value of 236 was achieved for a MLFRL using semiconductor optical amplifier (SOA) as the gain medium^[6]. However, the free spectral range (FSR) of the filter is limited to several tens of megahertz, making the filter unsuitable for broadband signal processing. Moreover, the above two methods of MPF have constrained tunability and reconfigurability. The most popular structure for MPF is based on the concept of discrete time optical processing of microwave

signals, including finite impulse response (FIR) and infinite impulse response (IIR) MPFs^[7]. IIR filters with active recirculation delay line can easily achieve relatively large Q-values, but again the FSR is limited to operate in incoherent regime^[8]. Different configurations of cascaded filters have been proposed to get the superposition of the transfer functions and increase the Q-values^[9-11]. But the FSR and bandwidth of the cascaded filters require rigid design and precise spectral alignment, which makes the filter less flexible. For a single FIR MPF, the Q-value is increased by using broadband optical source with larger bandwidth^[12] or by generating more optical frequency comb (OFC) spectral lines^[13]. Although the MPFs based on broadband optical source can achieve high Q-value of 634, it is still challenging to get a noise performance as good as the ones based on OFC^[14]. Supradeepa *et al.*^[13] further expanded the OFC generated via cascaded electro-optic modulators by the four-wave mixing in highly nonlinear fibers (HNLFs) but the largest Q was still no more than 50.

In this letter, a high-Q MPF based on the self-phase modulation (SPM) spectrum broadening and third-order dispersion (TOD) compensation is proposed and experimentally demonstrated. The chirp-free optical pulses from a mode-locking laser (MLL) are power amplified and fed to a length of HNLF. The nonlinear SPM effect generates new spectral lines and greatly broadens the optical spectrum envelope. In the case of zero TOD, the fulfilled MPF should have narrower passband bandwidth according to the principle of FIR filters. However, with broader optical spectrum, the TOD is no more negligible and will severely broaden the passband. When optical phase compensation is applied via a waveshaper to the modulated wideband OFC, the effect of TOD is eliminated. The final

Q-value of the proposed filter is 296. To the best of our knowledge, this is the highest Q-value for the MPFs which use optical combs as the source. We also present the tunability of the proposed MPF by changing the repetition frequency of the MLL.

The scheme of the high-Q MPF consists of two parts, as shown in Fig. 1. The first part is the SPM spectrum broadening and the second is the TOD compensation based on a waveshaper.

The chirp-free Gaussian optical pulses emitted from a MLL are used as the seed optical source. The pulses are first amplified by an erbium-doped fiber amplifier (EDFA) to a certain power and subsequently coupled into a length of HNLF. The dispersion of HNLF is negligible and the nonlinear interaction dominates, which produces a nonlinear phase modulation changed with the intensity of light and generates new frequency components. The largest nonlinear phase shift ϕ_{\max} in the process of SPM is given by^[15]

$$\phi_{\max} = \gamma P_0 L_{\text{eff}} \quad (1)$$

where γ and L_{eff} are the nonlinear coefficient and the effective length of the HNLF, respectively, and P_0 is the peak power of the pulses. For chirp-free Gaussian optical pulses with a given pulse width, the spectrum broadening factor is proportional to ϕ_{\max} . When the HNLF is fixed, larger optical power leads to broader optical spectrum and more spectral lines. As an example, we use a transform-limited Gaussian pulse with a full-width at half-maximum (FWHM) of 5 ps as the source, as shown in Fig. 2(a). The pulse repetition rate is 10.022 GHz and the average optical power is 23.52 dBm. Suppose the nonlinear coefficient of the HNLF is $10.8 \text{ (W} \cdot \text{km)}^{-1}$ and the length is 511 m. The calculated optical spectra before and after SPM are shown in Fig. 2(b). Obviously, the spectrum has been expanded considerably and the structure of fluctuation appears. The number of peaks under this optical power and pulse width is 8.

When the TOD and higher order dispersion are small enough to be neglected, the frequency transfer function of the MPF based on OFCs can be expressed as^[16]

$$H(\omega_{\text{RF}}) \propto \exp\left(j\frac{\theta_2}{2}\omega_{\text{RF}}^2\right) \sum_{r=0}^{N-1} I_r \exp(jr\Delta\Omega\omega_{\text{RF}}\theta_2), \quad (2)$$

where ω_{RF} is the microwave angular frequency, θ_2 is the second-order dispersion coefficient of the dispersive fiber, r is the sequence number of the comb lines, N is the total number, I_r is the power of each comb lines, and $\Delta\Omega$ is the repetition frequency of the OFC. The basic delay time in the transversal delay taps filters is determined by $\Delta\Omega\theta_2$. However, when the TOD is no longer negligible, the dispersion coefficient is dependent on the wavelength and the basic delay time between two adjacent taps is no longer uniformly spaced. In such case, suppose the TOD coefficient is θ_3 , and θ_3 is relatively small, within the bandwidth of the frequency combs, $\theta_3 r \Delta\Omega \omega_{\text{RF}}^2 \rightarrow 0$ and $\theta_3 \omega_{\text{RF}}^3 \rightarrow 0$. Then the

transfer function is rewritten as

$$H(\omega_{\text{RF}}) \propto \exp\left[j\left(\frac{\theta_2}{2}\omega_{\text{RF}}^2\right)\right] \sum_{r=0}^{N-1} \left\{ I_r \times \exp\left[j\left(r\Delta\Omega\omega_{\text{RF}}\theta_2 + \frac{\theta_3}{2}r^2\Delta\Omega^2\omega_{\text{RF}}\right)\right] \right\}. \quad (3)$$

The time delay between adjacent taps now is

$$T(r) = \Delta\Omega\theta_2 + \frac{\theta_3\Delta\Omega^2}{2} + \theta_3\Delta\Omega^2r. \quad (4)$$

As shown in Eq. (4), the tap delay is no longer fixed, but varies linearly with the tap wavelength. Within the band range of the frequency combs, different sections have different FSRs for the MPF, and the superposition of all the sections results in a broadened passband bandwidth.

Since the existence of TOD brings a cubic phase modulation on the spectrum of the modulated OFC, if a cubic phase modulation function with reversed coefficient is also applied, the effect of TOD can be eliminated. The cubic phase compensation function can be written as $\Phi(\Omega) = \chi(\Omega - \Omega_0)^3/6$ and $\chi = -\theta_3$, where Ω is the optical angular frequency and Ω_0 is the center angular frequency of the OFC. The commercially available waveshaper based on diffraction grating and liquid crystal on silicon (LCoS) is able to process wideband optical spectrum on both amplitude and phase. By designing a suitable amplitude and phase modulation function, a MPF with configurable passband shape and without distortion brought by TOD can be realized.

Experiments were carried out to verify the feasibility of the proposed filter based on the configuration shown in Fig. 1. The seed OFC was realized by a MLL (u²t TMLL1550), which had a repetition frequency of 10.022 GHz. The output optical spectrum is shown in Fig. 3(a), where 45 spectral lines can be seen within 10-dB power variation from the highest spectral power. The time domain pulse width at half magnitude was about 5 ps. This light source passed through an EDFA and the output power was 23.52 dBm. The HNLF used in the experiment had the same parameters as the ones we used in Fig. 2(b). The optical spectrum at the output of HNLF is shown in Fig. 3(b). It is obvious that the

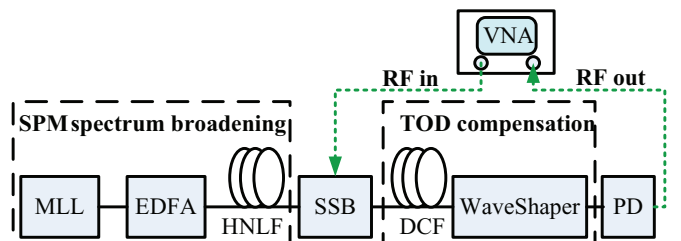


Fig. 1. Scheme of the proposed high-Q MPF. SSB, single-sideband modulation; VNA, vector network analyzer.

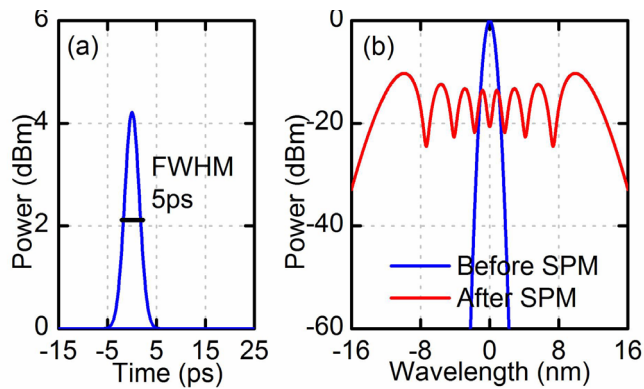


Fig. 2. (a) Gaussian-like optical pulse before SPM and (b) optical spectra before and after SPM.

optical spectrum has been greatly broadened, with 356 spectral lines in 10-dB power variation from the highest spectral power. The number of peaks in the fluctuation structure of the output spectrum is 8, which agrees well with the numerical calculation in Fig. 2 (b).

Then, the broadened OFC was fed into a dual-parallel Mach-Zehnder modulator to perform single-sideband modulation. A 16-km length of dispersion compensation fiber (DCF) was used as the dispersive device, which had a second-order dispersion of 1710 ps^2 at 1552.6 nm and a TOD of -8 ps^3 . The waveshaper (Finisar 1000S) had a wavelength operation range from 1530 to 1560 nm and the frequency resolution was 1 GHz. After being processed in the waveshaper, the light was launched into a photodetector (PD) with a bandwidth of 20 GHz.

When phase compensation was not applied in the waveshaper, the frequency combs without signal modulation before the PD was observed, as shown in Fig. 4(a). The measured MPF transfer function had a passband at about 9.5 GHz, but the bandwidth was greatly broadened, as shown in Fig. 4(b). Also shown in Fig. 4(b) is the calculation amplitude transfer function with the measured optical spectrum and the dispersion coefficients of the DCF. The two curves match well, which means the broadening of the passband is mainly due to the existence of TOD. The measured phase response of the filter is also shown in Fig. 4(b), which is

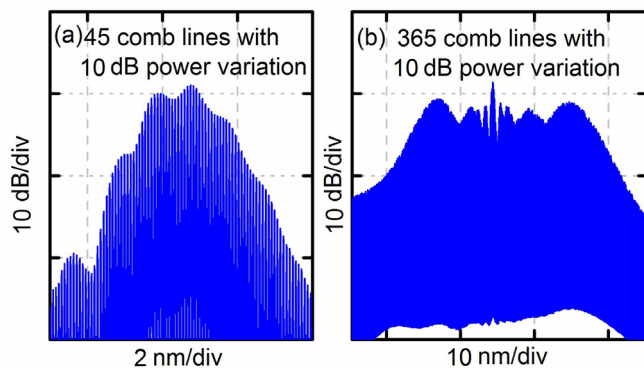


Fig. 3. (a) Optical spectrum directly from MLL and (b) optical spectrum after HNLF.

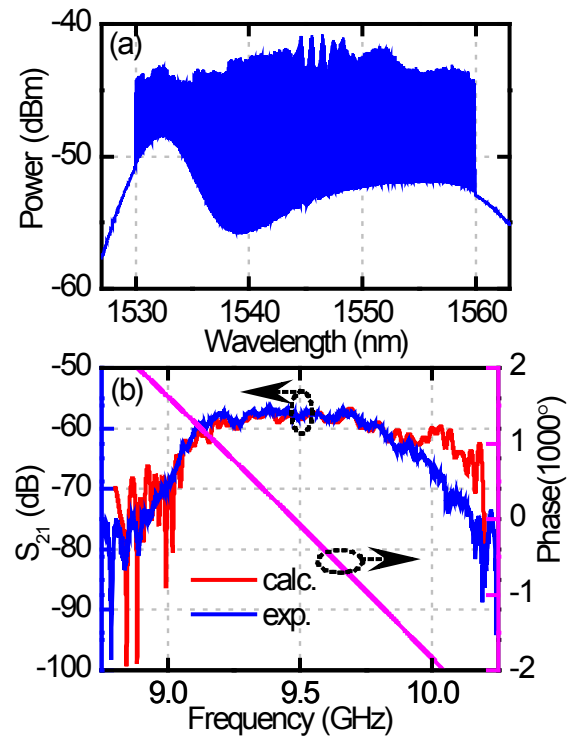


Fig. 4. (a) Optical spectrum before the PD and (b) filter transfer function without TOD compensation. Left axis, amplitude response, cal., calculation; exp., experiment; right axis, phase response in the experiment.

generally linear with the microwave frequency. But because of the existence of TOD, the quadratic coefficient of the phase curve is about 80.

Next, we applied the cubic phase modulation function via the waveshaper to the modulated optical signal. The optical spectrum after waveshaper is shown in Fig. 5(a). As the bandwidth of the optical spectrum was quite large, even tiny TOD would bring large phase change especially when the wavelength was far from the center, and thus large phase shift were needed in the waveshaper. However, the frequency resolution of the waveshaper was limited due to the dispersive ability of the diffraction grating, and as a result every single spectral line was controlled by more than one pixel. If the phase difference between two adjacent pixels is about $(2k + 1)\pi$ (k is an integer), interference will take place and the spectral line at that particular portion of the LCoS will be suppressed. That is the reason for the many gaps in Fig. 5(a) compared with Fig. 4(a). Although the number of usable spectral lines is decreased, it is still much larger than the number of spectral lines of MLL. The implemented filter transfer function after TOD compensation was measured in the experiment, as shown in Fig. 5(b). As a contrast, the theoretical calculation of the filter amplitude transfer function with the optical spectrum in Fig. 5(a) under zero TOD is also demonstrated. Again, excellent agreement between the two curves can be seen, which verifies the ability of

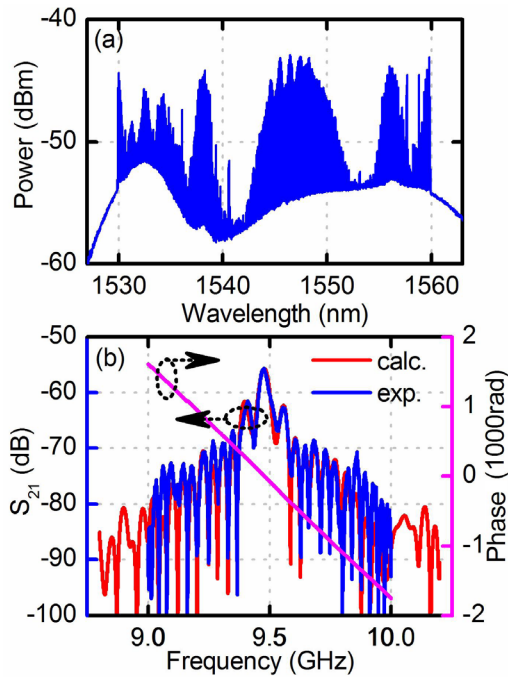


Fig. 5. (a) Optical spectrum before the PD and (b) filter transfer function with TOD compensation. Left axis, amplitude response, cal., calculation; exp., experiment; right axis, phase response in the experiment.

TOD compensation. The center frequency of the filter is 9.476 GHz, with a 3-dB bandwidth of 32 MHz. The Q-value is 296. The phase response of the filter is also measured and is shown in Fig. 5(b). The linear relation between the phase and the frequency is improved, with a quadratic coefficient of 18 in the passband. The Q-value and the linearity of the phase-frequency curve would be further improved if a waveshaper with better frequency resolution could be available.

As shown in Eq. (2), the central frequency of the MPF is determined by the repetition frequency of the MLL and the second-order dispersion coefficient of the dispersive fiber when the TOD is compensated. In the experiment, we changed the repetition frequency to show the tunability of the fulfilled MPF. The results are shown in Fig. 6. The repetition frequency is changed from 10.6 to 9.8 GHz, with 0.2 GHz each step. Correspondingly, the filter center frequency is tuned from 9.045 to 9.784 GHz. The tuning range is 740 MHz. The 3-dB bandwidth of the filter stays around 32 MHz, with a variation range of less than 1 MHz.

In conclusion, we propose and experimentally demonstrate a scheme of high-Q MPF using the techniques of SPM spectrum broadening and TOD compensation. In the experiment, a wideband OFC with 365 spectral lines within 10-dB power variation from the highest spectral power is obtained. The effect of TOD which greatly broadens the passband of the MPF is investigated in

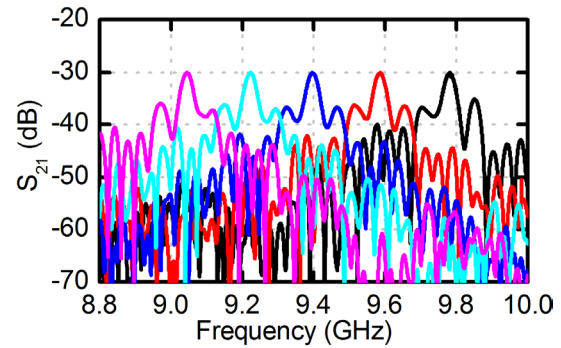


Fig. 6. Tunability of the high-Q MPF.

the experiment. When a cubic phase modulation function with a coefficient reverse to the TOD coefficient is applied through a waveshaper, the narrow passband can be recovered. Experimental results have demonstrated a MPF with the FSR of 9.476 GHz and Q-value as high as 296. The central frequency of the proposed MPF can also be tuned within a range of 700 MHz.

This work was supported in part by the National Key Basic Research Program of China (Nos. 2012CB315603 and 2012CB315604) and the National Natural Science Foundation of China (Nos. 61025004, 61032005, and 61321004).

References

1. J. Capmany and D. Novak, *Nat. Photon.* **6**, 319 (2007).
2. J. Yao, *J. Lightwave Technol.* **3**, 314 (2009).
3. Y. Yu, X. Zheng, H. Zhang, and B. Zhou, *Chin. Opt. Lett.* **11**, 120601 (2013).
4. D. Zhang, X. Feng, and Y. Huang, *Chin. Opt. Lett.* **10**, 21302 (2012).
5. B. V. Rodríguez, M. A. Piqueras, and J. Martí, *Opt. Lett.* **1**, 23 (2007).
6. E. Xu, F. Wang, and P. Li, *Optoelectron. Lett.* **9**, 97 (2013).
7. J. Capmany, B. Ortega, D. Pastor, and S. Sales, *J. Lightwave Technol.* **2**, 702 (2005).
8. Y. Yu, E. Xu, J. Dong, L. Zhou, X. Li, and X. Zhang, *Opt. Express* **24**, 25271 (2010).
9. J. Capmany, J. Mora, B. Ortega, and D. Pastor, *Opt. Lett.* **17**, 2299 (2005).
10. N. You and R. A. Minasian, *Electron. Lett.* **24**, 2125 (1999).
11. E. Xu, X. Zhang, L. Zhou, Y. Zhang, Y. Yu, X. Li, and D. Huang, *Opt. Lett.* **8**, 1242 (2010).
12. X. Xue, X. Zheng, H. Zhang, and B. Zhou, in *Proceedings of OFC 2013 OTu2H.2* (2013).
13. V. R. Supradeepa, C. M. Long, Rui Wu, F. Ferdous, E. Hamidi, D. E. Leaird, and A. M. Weiner, *Nat. Photon.* **3**, 186 (2012).
14. M. Song, V. Torres-Company, and A. M. Weiner, *IEEE Photon. Technol. Lett.* **14**, 1236 (2012).
15. G. P. Agrawal, *Nonlinear Fiber Optics* (Springer, Berlin, 2000).
16. E. Hamidi, D. E. Leaird, and A. M. Weiner, *IEEE Trans. Microwave Theory* **11**, 3269 (2010).